Journal of Organometallic Chemistry 695 (2010) 2441–2446

Contents lists available at ScienceDirect

Journal of Organometallic Chemistry

journal homepage: www.elsevier.com/locate/jorganchem

m-Ferrocenylbenzoate-bridged lanthanide coordination polymers: Syntheses, structures, electrochemical and magnetic properties

Bin-Qiu Liu [a,b], Peng-Fei Yan [a,b], Ju-Wen Zhang [a,b], Peng Chen [a,b], Guang-Ming Li [a,b,*]

[a] *Key Laboratory of Functional Inorganic Material Chemistry (Heilongjiang University), Ministry of Education, PR China*
[b] *School of Chemistry and Materials Science, Heilongjiang University, No. 74, Xuefu Road, Nangang District, Harbin 150080, PR China*

ARTICLE INFO

Article history:
Received 26 February 2010
Received in revised form
25 June 2010
Accepted 14 July 2010
Available online 21 July 2010

Keywords:
m-Ferrocenylbenzoic acid
Lanthanide
Synthesis
Structure
Electrochemistry
Magnetism

ABSTRACT

A series of *m*-ferrocenylbenzoate [*m*-ferrocenylbenzoate = *m*-$NaOOCH_4C_6Fc$, Fc = $(\eta^5\text{-}C_5H_5)Fe(\eta^5\text{-}C_5H_4)$] lanthanide coordination polymers, namely $[Ln(\mu_2\text{-}OOCH_4C_6Fc)(\eta^2\text{-}OOCH_4C_6Fc)(\mu_2\text{-}\eta^2\text{-}OOCH_4C_6Fc)(CH_3OH)_2]_n$ [Ln = La (**1**), Pr (**2**), Nd (**3**), Sm (**4**) and Gd (**5**)], have been synthesized by reactions of *m*-ferrocenylbenzoate with $Ln(NO_3)_3\cdot nH_2O$. X-ray crystallographic analyses reveal that **1**, **2** and **5** are essentially isostructural with unique one-dimensional linear chain structure. Three types of coordination modes for *m*-ferrocenylbenzoate are observed in the unit structure which consists of the eight-membered metallacycle $Ln_2(COO)_2$ and the rhomboid Ln_2O_2. Electrochemical studies indicate that **1**–**5** exhibit a reversible redox wave of Fe^{II}/Fe^{III} and the half-wave potentials of **1**–**5** are slightly more positive than that of *m*-ferrocenylbenzoic acid. Magnetic investigations show that an antiferromagnetic interaction between Gd(III) ions exists in **5**.

1. Introduction

Lanthanide complexes have attracted increasing attention due to their interesting topological structures and potential applications in electrochemistry, magnetism, photochemistry and catalysis [1–4]. On the basis of the strong coordination ability and versatile coordination modes of carboxylate group, carboxylate lanthanide complexes have been studied extensively pertaining to their unique topological structures and excellent physicochemical properties [5–13]. It is known that the coordination modes of carboxylate group usually include the following: (i) coordinating terminal monodentate to one metal ion, (ii) chelating bidentate to one metal ion, (iii) bridging bidentate to two metal ions in a *syn*–*syn*, *syn*–*anti* or *anti*–*anti* fashion and (iv) bridging and chelating tridentate to two metal ions [14–17].

However, there are few ferrocenecarboxylate lanthanide complexes known. In 2002, Wong and co-workers reported the first ferrocenecarboxylate lanthanide complex $[Eu_2(Fcdc)_3(H_2O)_4]_n\cdot nH_2O$ ($FcdcH_2$ = 1,1′-ferrocenedicarboxylic acid) featuring a two-dimensional interlinking zigzag-chain network [18]. Hou and co-workers synthesized two ferrocenecarboxylate-bridged lanthanide dimers $[Gd_2(\mu_2\text{-}OOCFc)_2(OOCFc)_4(MeOH)_2(H_2O)_2]\cdot 2MeOH\cdot 2H_2O$ and $[Nd_2(\mu_2\text{-}OOCFc)_2(OOCFc)_4(H_2O)_4]\cdot 2MeOH\cdot H_2O$ and discussed their magnetic properties in 2003 [19]. Moreover, Hou and co-workers also prepared three one-dimensional polymers $[Ln(\eta^2\text{-}OOCH_4C_2OCFc)(\mu_2\text{-}\eta^2\text{-}OOCH_4C_2OCFc)_2(H_2O)_2]_n$ (Ln = La, Ce and Pr) and investigated their electrochemical, magnetic and fluorescent properties in 2006 [20]. Recently, Mereacre and co-workers reported the first 3d–4f multinuclear complex containing organometallic ferrocene $[Mn_4Nd_4(OH)_4(Fcdc)_2(Piv)_8(bdea)_4]\cdot H_2O$ [PivH = $(CH_3)_3CCOOH$, $bdeaH_2$ = *N*-butyldiethanolamine] and described its magnetic properties [21]. We obtained two *p*-ferrocenylbenzoate lanthanide complexes $\{[Ln(OOCH_4C_6Fc)_2(\mu_2\text{-}OOCH_4C_6Fc)_2(H_2O)_2](H_3O)\}_n$ (Ln = Ce and Pr) possessing a unique one-dimensional chain in 2009 [22]. Herein, we present the syntheses, structures, electrochemical and magnetic properties of an array of *m*-ferrocenylbenzoate lanthanide coordination polymers.

2. Experimental

2.1. Materials and physical measurements

All chemicals were commercially available. *m*-Ferrocenylbenzoate sodium was prepared according to the literature method [23]. Elemental analyses (C and H) were carried out on

---

* Corresponding author. School of Chemistry and Materials Science, Heilongjiang University, No. 74, Xuefu Road, Nangang District, Harbin 150080, PR China. Tel.: +86 451 86608428; fax: +86 451 86604799.
E-mail address: gmli_2000@163.com (G.-M. Li).

0022-328X/$ – see front matter © 2010 Elsevier B.V. All rights reserved.
doi:10.1016/j.jorganchem.2010.07.010

Table 1
Crystallographic data and structural refinement for **1**, **2** and **5**.

	1	**2**	**5**
Formula	$C_{53}H_{47}Fe_3O_8La$	$C_{53}H_{47}Fe_3O_8Pr$	$C_{53}H_{47}Fe_3O_8Gd$
Formula weight	1118.37	1120.37	1136.71
Temperature (K)	291(2)	291(2)	296(2)
Wavelength (Å)	0.71073	0.71073	0.71073
Crystal system	Triclinic	Triclinic	Triclinic
Space group	$P-1$	$P-1$	$P-1$
a (Å)	9.898(3)	9.850(3)	9.894(6)
b (Å)	13.707(5)	13.689(5)	14.032(8)
c (Å)	16.916(7)	16.840(7)	17.702(10)
α (°)	93.077(14)	93.014(16)	110.987(9)
β (°)	94.280(13)	94.144(14)	90.917(9)
γ (°)	95.394(11)	95.376(14)	96.936(10)
V (Å^3)	2274.2(14)	2250.8(15)	2273(2)
Z	2	2	2
Calculated density (g cm^{-3})	1.633	1.653	1.661
μ (mm^{-1})	1.914	2.068	2.434
F(000)	1128	1132	1142
θ range for data collection (°)	2.99–25.00	2.99–25.00	1.57–24.34
Reflections collected/unique	17895/7964	17652/7812	12158/7337
R_{int}	0.0458	0.0318	0.0480
R_1, wR_2 ($I > 2\sigma(I)$)	0.0421, 0.1120	0.0344, 0.1086	0.0783, 0.2015
R_1, wR_2 (all data)	0.0609, 0.1410	0.0424, 0.1157	0.1061, 0.2193
GOF on F^2	1.046	1.097	1.007

a Perkin–Elmer 2400 analyzer. IR spectra were recorded on a Perkin–Elmer 60000 spectrophotometer with KBr disks in the 370–4000 cm^{-1} region. UV spectra were performed on a UV-3600 spectrophotometer. Magnetic data were measured on a Quantum Design MPMSXL7 (SQUID) magnetometer. The diamagnetic corrections were made by using Pascal's constants.

2.2. Electrochemistry

Cyclic voltammetry (CV) and differential pulse voltammetry (DPV) studies were carried out with a CHI650C electrochemical analyzer utilizing the three-electrode configuration of a glassy carbon (3 mm diameter) working electrode, a Pt auxiliary electrode and a Ag/AgCl reference electrode. The Ag/AgCl reference electrode was AgCl-coated Ag wire obtained via anodic electrolysis of the silver wire in KCl (0.1 mol L^{-1}) and separated from the test solution by a salt bridge containing acetonitrile solution of n-Bu_4NPF_6 (0.1 mol L^{-1}). The working electrode was polished with 30–50 nm alumina slurry on the polishing cloth and rinsed copiously with water and ethanol in an ultrasonic bath prior to use. The measurements were performed in DMF solution containing n-Bu_4NPF_6 (0.1 mol L^{-1}) as supporting electrolyte at room temperature. The pure nitrogen gas was used to sparge the DMF solution in which the three electrodes were placed. The concentration of all samples for CV curves is 0.5, 1 and 1.5 mmol L^{-1}, respectively. CV curves were recorded at scan rates of 20, 50 and 100 mV s^{-1} from 0 to 0.85 V. The concentration of all samples for DPV curves is 1 mmol L^{-1}. DPV curves were recorded at a scan rate of 20 mV s^{-1} with pulse width of 50 ms and sample width of 16.7 ms.

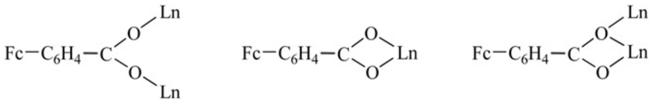

Scheme 2. Three types of coordination modes of m-ferrocenylbenzoate in **1**, **2** and **5**.

2.3. Syntheses of [Ln(μ_2-$OOCH_4C_6Fc$)(η^2-$OOCH_4C_6Fc$)(μ_2-η^2-$OOCH_4C_6Fc$)(CH_3OH)$_2$]$_n$ [Ln = La (**1**), Pr (**2**), Nd (**3**), Sm (**4**) and Gd (**5**)]

A methanol solution (16 mL) of m-$NaOOCH_4C_6Fc$ (0.3 mmol) was added dropwise to an aqueous solution (16 mL) of Ln $(NO_3)_3 \cdot nH_2O$ (0.1 mmol) at room temperature. The resulting solutions were stored in the dark at ambient temperature. Orange crystals were obtained after two weeks.

Compound **1**: yield: 40%. Elementary anal. (wt%) Calc. for $C_{53}H_{47}Fe_3LaO_8$ (1118.37): C, 56.92; H, 4.24. Found: C, 57.13; H, 4.16. IR (cm^{-1}, KBr): 3432 (m), 3092 (w), 1521 (s), 1465 (s), 1404 (s), 1271 (m), 1105 (w), 1017 (m), 1001 (w), 915 (w), 814 (m), 772 (s), 722 (m), 691 (w), 495 (m), 441 (w). UV (CH_3OH, nm): 223, 281.

Compound **2**: yield: 45%. Elementary anal. (wt%) Calc. for $C_{53}H_{47}Fe_3PrO_8$ (1120.37): C, 56.82; H, 4.23. Found: C, 57.21; H, 4.18. IR (cm^{-1}, KBr): 3435 (m), 3091 (w), 1523 (s), 1466 (s), 1403 (s), 1271 (m), 1105 (w), 1017 (m), 1001 (w), 914 (w), 818 (m), 772 (s), 722 (m), 690 (w), 493 (m), 443 (w). UV (CH_3OH, nm): 223, 280.

Compound **3**: yield: 55%. Elementary anal. (wt%) Calc. for $C_{53}H_{47}Fe_3NdO_8$ (1123.71): C, 56.65; H, 4.22. Found: C, 56.95; H, 4.17. IR (cm^{-1}, KBr): 3427 (m), 3092 (w), 1543 (s), 1467 (s), 1406 (s), 1271 (m), 1105 (w), 1017 (m), 1000 (w), 916 (w), 820 (m), 771 (s), 722 (m), 690 (w), 494 (m), 442 (w). UV (CH_3OH, nm): 224, 281.

Compound **4**: yield: 45%. Elementary anal. (wt%) Calc. for $C_{53}H_{47}Fe_3SmO_8$ (1129.83): C, 56.34; H, 4.19. Found: C, 56.67; H, 4.16. IR (cm^{-1}, KBr): 3428 (m), 3092 (w), 1547 (s), 1467 (s), 1408 (s), 1271 (m), 1106 (w), 1017 (m), 1001 (w), 916 (w), 821 (m), 771 (s), 723 (m), 691 (w), 494 (m), 445 (w). UV (CH_3OH, nm): 222, 281.

Compound **5**: yield: 55%. Elementary anal. (wt%) Calc. for $C_{53}H_{47}Fe_3GdO_8$ (1136.71): C, 56.00; H, 4.17. Found: C, 57.17; H, 4.19. IR (cm^{-1}, KBr): 3436 (m), 3093 (w), 1526 (s), 1467 (s), 1411 (s), 1271 (m), 1105 (w), 1017 (m), 1001 (w), 914 (w), 813 (m), 771 (s), 725 (m), 689 (w), 496 (m), 443 (w). UV (CH_3OH, nm): 223, 281.

2.4. X-ray structure determination

Crystallographic data for **1**, **2** and **5** were collected on a Rigaku Raxis-Rapid X-ray diffractometer with graphite-monochromated Mo Kα radiation. The structures were solved by direct methods using the program SHELXS-97 and all non-hydrogen atoms were refined anisotropically on F^2 by the full-matrix least-squares technique using the SHELXL-97 crystallographic software package

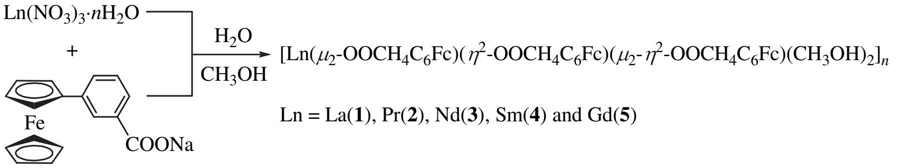

Scheme 1. Syntheses of **1**–**5**.

[24,25]. Pertinent crystallographic data and structural refinement for **1**, **2** and **5** are listed in Table 1.

3. Results and discussion

3.1. Syntheses

The *m*-ferrocenylbenzoate lanthanide coordination polymers **1**–**5** were synthesized by slowly diffusing a methanol solution of *m*-ferrocenylbenzoate sodium into a water solution of $Ln(NO_3)_3\cdot nH_2O$ (Scheme 1).

3.2. Description of structures

X-ray crystallographic analysis reveals that **1**, **2** and **5** are essentially isostructural. Therefore, we will restrict our description to **1** and only discuss pertinent points for **2** and **5**, where appropriate. Coordination polymer **1** crystallizes in the space group *P*–1. *m*-Ferrocenylbenzoates bridge La(III) ions forming a one-dimensional linear chain with a slight twist (the La···La···La angles are all 173.07°) by three types of coordination modes (Scheme 2), *viz.* bidentate-bridging (μ_2-OOCH$_4$C$_6$Fc), bidentate-chelating (η^2-OOCH$_4$C$_6$Fc) and tridentate-bridging-chelating (μ_2-η^2-OOCH$_4$C$_6$Fc) (Fig. 1a), which are different from those of the reported ferrocenecarboxylate complexes [22,26–29]. The 1D linear chain is composed of an eight-membered metallacycle La$_2$(COO)$_2$ and a rhomboid La$_2$O$_2$ [20,30] arranged alternatively (Fig. 1b). In the rhomboid, two oxygen atoms are from two μ_2-η^2-OOCH$_4$C$_6$Fc units. The dimension of the rhomboid is 2.528(4) × 2.921(4) Å and the internal angles are 67.59 (O3–La1–O3A) and 112.41° (La1–O3–La1), respectively. The eight-membered metallacycle with two La(III) centers is formed by two μ_2-OOCH$_4$C$_6$Fc units acting as a *syn*–*anti* mode. The *syn*–*anti* bonding mode of carboxylates from the μ_2-OOCH$_4$C$_6$Fc units leads to a chair conformation of the eight-membered metallacycle [31]. The dihedronal angle between the O5La1O6 and O3La1O3A planes is 44.40°. The neighboring La···La distances in the chain are 4.534 Å and 5.382 Å, alternately (Table 2), which is different from the identical Ln···Ln distances in the reported *p*-ferrocenylbenzoate lanthanide complexes [22]. This is attributed to that two different coordination modes of μ_2-OOCH$_4$C$_6$Fc and μ_2-η^2-OOCH$_4$C$_6$Fc for *m*-ferrocenylbenzoates bridge between neighboring La(III) ions in **1**, alternately. Whereas the *p*-ferrocenylbenzoates bridge Ln(III) ions only by the μ_2-OOCH$_4$C$_6$Fc coordination mode in the reported *p*-ferrocenylbenzoate lanthanide complexes.

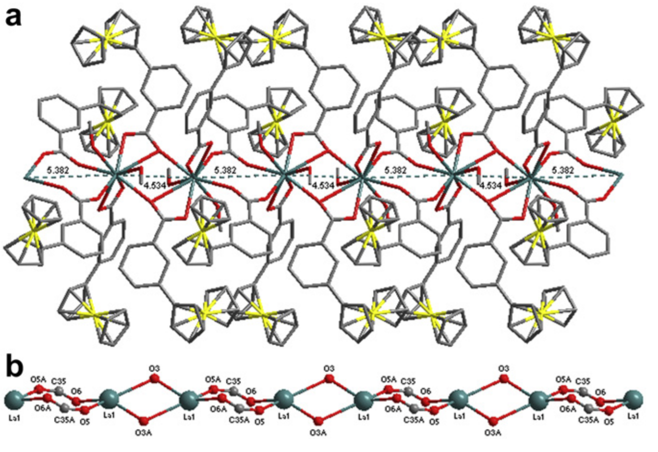

Fig. 1. (a) 1D chain structure of **1** (all hydrogen atoms are omitted for clarity). (b) Eight-membered metallacycle La$_2$(COO)$_2$ and rhomboid La$_2$O$_2$ of **1** arranged alternatively.

Table 2
Selected bond distances (Å) for **1**, **2** and **5**.

	1 (La)	**2** (Pr)	**5** (Gd)
Ln1–O1	2.568(4)	2.524(3)	2.479(10)
Ln1–O2	2.590(4)	2.547(3)	2.308(9)
Ln1–O3	2.921(4)	2.932(3)	3.375
Ln1–O3A	2.528(4)	2.490(3)	2.454(9)
Ln1–O4	2.486(4)	2.435(3)	2.537(9)
Ln1–O5	2.422(4)	2.383(3)	2.465(10)
Ln1–O6	2.445(4)	2.412(3)	2.317(8)
Ln1–O7	2.645(4)	2.610(3)	2.294(9)
Ln1–O8	2.568(4)	2.536(4)	2.349(8)
Ln–O (*av.*)	2.575	2.541	2.509
Ln···Ln	4.534/5.382	4.531/5.336	4.806/5.092

In **1**, each La(III) ion is nine-coordinated by nine oxygen atoms, of which two are from two μ_2-OOCH$_4$C$_6$Fc units, two are from one η^2-OOCH$_4$C$_6$Fc unit, three are from two μ_2-η^2-OOCH$_4$C$_6$Fc units and two are from two methanol molecules (Fig. 2). The coordination polyhedron around the La(III) ion can be described as a distorted monocapped square antiprism. The La–O distances are in the range of 2.422(4)–2.921(4) Å (Table 2). The average bond distance of La–O is 2.575 Å. In **2**, the Pr–O distances are in the range of 2.383 (3)–2.932(3) Å. The average bond distance of Pr–O is 2.541 Å. In **5**, the Gd–O distances are in the range of 2.308(9)–3.375 Å. The average bond distance of Gd–O is 2.509 Å. It should be noticed that the Gd1–O3 distance of 3.375 Å is much longer than La1–O3 [2.921 (4) Å] and Pr1–O3 [2.932(3) Å], which indicates that the Gd1–O3 bond has become very weak in **5**. The change trend of the Ln–O distances (except Gd1–O4, Gd1–O5 and Ln1–O3), average Ln–O

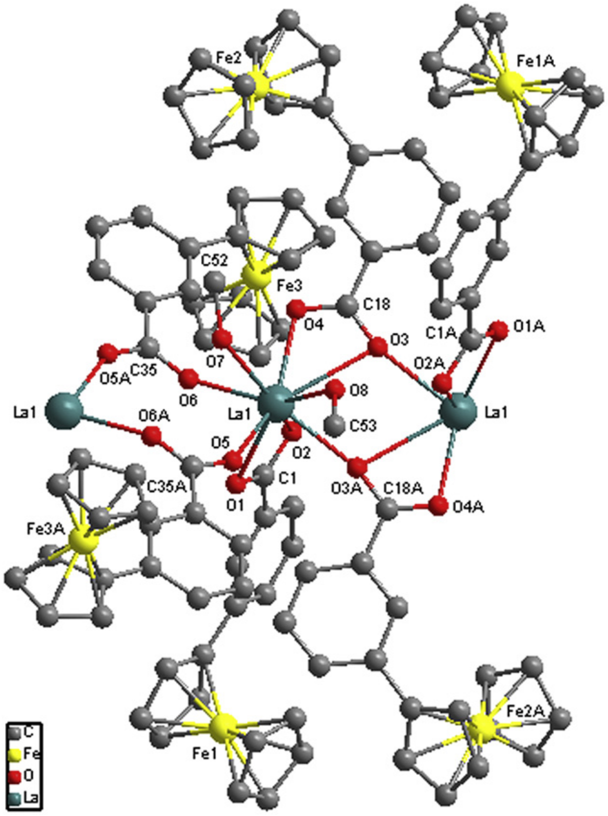

Fig. 2. Unit structure of **1** (all hydrogen atoms are omitted for clarity).

Table 3
Structural parameters of three types of coordination modes for *m*-$OOCH_4C_6Fc$ in **1**, **2** and **5**.

		Bite angles (°)	Dihedronal angle 1 (°)	Dihedronal angle 2 (°)	Dihedronal angle 3 (°)	Range/average (Å)[a]	Unsubstituted /substituted ring (Å)[b]
1	μ_2-$OOCH_4C_6Fc$ (Fe3)	123.54	5.42	9.44	3.63	1.990–2.078/2.034	1.405/1.428
	η^2-$OOCH_4C_6Fc$ (Fe1)	120.36	3.35	7.16	2.49	2.017–2.054/2.036	1.410/1.414
	μ_2-η^2-$OOCH_4C_6Fc$ (Fe2)	120.93	5.06	47.02	0.50	2.024–2.073/2.048	1.415/1.420
2	μ_2-$OOCH_4C_6Fc$ (Fe3)	123.37	4.53	8.81	3.44	2.011–2.061/2.036	1.395/1.423
	η^2-$OOCH_4C_6Fc$ (Fe1)	120.32	3.17	6.58	2.91	2.021–2.047/2.034	1.407/1.409
	μ_2-η^2-$OOCH_4C_6Fc$ (Fe2)	120.34	4.99	46.97	0.70	2.020–2.046/2.033	1.403/1.414
5	μ_2-$OOCH_4C_6Fc$ (Fe3)	123.19	7.08	12.13	2.36	2.022–2.049/2.033	1.408/1.412
	η^2-$OOCH_4C_6Fc$ (Fe1)	118.14	9.78	7.42	3.80	1.963–2.043/2.012	1.352/1.381
	μ_2-η^2-$OOCH_4C_6Fc$ (Fe2)	121.90	7.37	25.51	1.44	2.003–2.051/2.026	1.403/1.404

[a] The distances of Fe–C_{ring} within the ferrocenyl fragments.

[b] The C–C mean distances within the two cyclopentadienyl rings.

distances and Ln···Ln distances (except Gd···Gd) basically follows the law of lanthanide contraction for **1**, **2** and **5**. However, the distances of Gd1–O4, Gd1–O5 and Gd···Gd are against the law of lanthanide contraction. Moreover, the bond distances of Ln1–O3 gradually increase along with the decrease of the size of the lanthanide ions for **1**, **2** and **5**. It results from the cooperative effect of the decrease of the size of the lanthanide ions and the increasing steric effect of the *m*-ferrocenylbenzoates along with the decrease of the size of the lanthanide ions.

Furthermore, the structural parameters of three types of coordination modes for *m*-$OOCH_4C_6Fc$ in **1** are different from each other (Table 3). For μ_2-$OOCH_4C_6Fc$ (Fe3), η^2-$OOCH_4C_6Fc$ (Fe1) and μ_2-η^2-$OOCH_4C_6Fc$ (Fe2), the bite angles of O5–C35A–O6A, O1–C1–O2 and O3–C18–O4 of the carboxylate groups are 123.54, 120.36 and 120.93°, respectively (Fig. 2). The dihedronal angle 1 between the carboxylate group and linking phenyl ring planes is 5.42, 3.35 and 5.06°, respectively. The dihedronal angle 2 between the phenyl ring and linking cyclopentadienyl ring planes is 9.44, 7.16 and 47.02°, respectively. The dihedronal angle 3 between the cyclopentadienyl ring planes in each ferrocenyl fragment is 3.63, 2.49 and 0.50°, respectively. Meanwhile, within the ferrocenyl fragments, the distances of Fe–C_{ring} are in the range of 1.990–2.078 Å (average 2.034 Å) for μ_2-$OOCH_4C_6Fc$, 2.017–2.054 Å (average 2.036 Å) for η^2-$OOCH_4C_6Fc$ and 2.024–2.073 Å (average 2.048 Å) for μ_2-η^2-$OOCH_4C_6Fc$. The C–C mean distances within the two cyclopentadienyl rings are in the normal range. For the unsubstituted and substituted rings, the C–C mean distances are 1.405 and 1.428 Å in μ_2-$OOCH_4C_6Fc$, 1.410 and 1.414 Å in η^2-$OOCH_4C_6Fc$ as well as 1.415 and 1.420 Å in μ_2-η^2-$OOCH_4C_6Fc$, which are similar to those (1.380 and 1.426 Å) of the reported ferrocenoylacetone-containing polymer [32]. Obviously, the differences of the structural parameters of three types of coordination modes for *m*-$OOCH_4C_6Fc$ in each coordination polymer (Table 3) are ascribed to the steric effect of the *m*-ferrocenylbenzoates [33].

3.3. Electrochemical properties

High redox ability is one of the unique features of ferrocene and its derivatives [20,30,34]. Thus, the electrochemical properties of compounds containing ferrocenyl group have been extensively studied.

The electrochemical behaviors of **1**–**5**, *m*-$HOOCH_4C_6Fc$ and ferrocene were comparatively investigated by cyclic voltammetry (CV) and differential pulse voltammetry (DPV) in DMF solution of *n*-Bu_4NPF_6 (0.1 mol L^{-1}). The CV and DPV curves of **1**, *m*-$HOOCH_4C_6Fc$ and ferrocene are shown in Fig. 3. The CV and DPV curves of **2**–**5** are similar to those of **1**. The electrochemical data for all compounds are summarized in Table 4. According to the CV and DPV results, all compounds exhibit a reversible redox wave in CV curves (Fig. 3a) and a single peak in DPV curves (Fig. 3b). Obviously, the observed redox peaks of **1** and *m*-$HOOCH_4C_6Fc$ correspond to the redox processes of the ferrocenyl moieties.

In contrast to free ferrocene, the half-wave potential ($E_{1/2}$) of *m*-$HOOCH_4C_6Fc$ is shifted to more positive potential. It is because that the electron-donating ability of the conjugated phenyl ring group just partially serves to counteract the electron-withdrawing inductive effect of the carboxylate group, which makes the half-wave potential of *m*-$HOOCH_4C_6Fc$ raise above that of free ferrocene [35,36]. Furthermore, the half-wave potentials of **1**–**5** are slightly more positive (*ca.* 10 mV) than that of *m*-$HOOCH_4C_6Fc$. This is

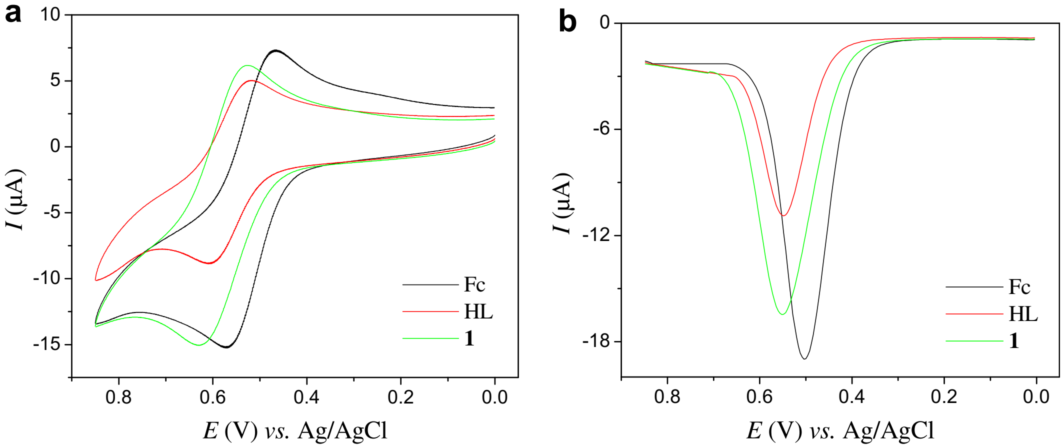

Fig. 3. Cyclic voltammograms (sample concentration: 1 mmol L^{-1}; scan rate: 100 mV s^{-1}) (a) and differential pulse voltammograms (b) of **1**, *m*-$HOOCH_4C_6Fc$ (HL) and ferrocene (Fc).

Table 4
Electrochemical data of **1**–**5**, *m*-$HOOCH_4C_6Fc$ (HL) and ferrocene (Fc) (E, V vs. Ag/AgCl; I, μA).

	CV[a]							DPV						
	E_{pa}	I_{pa}	E_{pc}	I_{pc}	I_{pc}/I_{pa}	ΔE_p[b]	$E_{1/2}$[b]	E_{pa}	I_{pa}	E_{pc}	I_{pc}	I_{pc}/I_{pa}	ΔE_p[b]	$E_{1/2}$[b]
Fc	0.572	−12.81	0.465	9.228	0.720	0.107	0.518	0.504	−17.80	0.542	15.22	0.855	0.038	0.523
HL	0.608	−6.754	0.519	4.336	0.642	0.089	0.564	0.548	−9.773	0.586	7.204	0.737	0.038	0.567
1 (La)	0.630	−12.23	0.527	7.582	0.620	0.103	0.578	0.552	−14.99	0.602	12.33	0.822	0.050	0.577
2 (Pr)	0.632	−12.84	0.519	7.918	0.617	0.113	0.576	0.552	−15.27	0.598	12.60	0.825	0.046	0.575
3 (Nd)	0.631	−12.63	0.520	7.785	0.616	0.111	0.576	0.548	−15.21	0.594	13.18	0.866	0.046	0.571
4 (Sm)	0.641	−13.12	0.521	7.867	0.600	0.120	0.581	0.556	−14.98	0.602	12.80	0.854	0.046	0.579
5 (Gd)	0.649	−11.74	0.533	7.150	0.609	0.116	0.591	0.568	−13.87	0.610	11.83	0.853	0.042	0.589

[a] Sample concentration: 1 mmol L^{-1}; scan rate: 100 mV s^{-1}.
[b] $\Delta E_p = E_{pa} - E_{pc}$; $E_{1/2} = (E_{pa} + E_{pc})/2$.

similar to the previous reports [37–40]. It is apparent that the electron-withdrawing nature of the coordinated lanthanide ions in **1**–**5** makes the oxidations of the ferrocenyl moieties become difficult. The change of *ca.* 10 mV indicates that the lanthanide ions have a small influence on the oxidations of the ferrocenyl moieties in **1**–**5**, which may be attributed to the relatively long charge-transfer distance between the lanthanide ions and Fe^{II} ion by the carboxylate group, phenyl ring and cyclopentadienyl ring. In short, the phenyl ring groups, carboxylate groups and lanthanide ions cooperatively influence the oxidation potentials of **1**–**5**. As seen in Table 4, the half-wave potentials of **1**–**3** (light lanthanide coordination polymers) are basically similar to each other. However, the half-wave potentials of **4** and **5** (middle lanthanide coordination polymers) are more positive than those of **1**–**3** and the half-wave potential of **5** is obviously more positive than that of **4**. The change trend of the half-wave potentials of **1**–**5** is basically consistent with that of the structural parameters for **1**, **2** and **5** (Table 2).

The current and potential values of the 1st–10th cycle for **1** almost remain invariable. The 1st–10th cycles of **2**–**5** are similar to that of **1**. The results of the 1st–10th cycles for **1**–**5** suggest that the electrochemical properties of **1**–**5** are stable. The CV measurements of **1**–**5** and ferrocene at different concentrations (0.5/1/1.5 mmol L^{-1}) and scan rates (20/50/100 mV s^{-1}) were carried out. The results indicate that the CV curves of **1**–**5** are similar to those of ferrocene at different measurement condition, which further shows that the redox processes of **1**–**5** are reversible.

3.4. Magnetic properties

The variable-temperature magnetic susceptibility of **5** was measured in the temperature range of 2–300 K at an applied field of 1000 Oe. The χ_m vs. T and the $\chi_m T$ vs. T plots are shown in Fig. 4. The $\chi_m T$ value at 300 K is 7.94 emu mol^{-1} K, which is slightly higher than the theoretical value (7.88 emu mol^{-1} K) for one isolated Gd(III) ($S = 7/2$, $g = 2$) ion [2]. From 300 K to 2 K, $\chi_m T$ decreases gradually to a minimum of 2.53 emu mol^{-1} K. The $\chi_m T$ vs. T curve indicates that an antiferromagnetic coupling between paramagnetic centers exists in **5**. Such an antiferromagnetic behavior should be originated from the antiferromagnetic interaction between Gd(III) ions through carboxylate bridges. The antiferromagnetic behavior of **5** is different from the weak ferromagnetic property of the reported *p*-ferrocenylbenzoate gadolinium complex [22], which may be attributed to the different bridging modes of carboxylate groups in **5** (μ_2-$OOCH_4C_6Fc$ and μ_2-η^2-$OOCH_4C_6Fc$) and the reported *p*-ferrocenylbenzoate gadolinium complex (μ_2-$OOCH_4C_6Fc$).

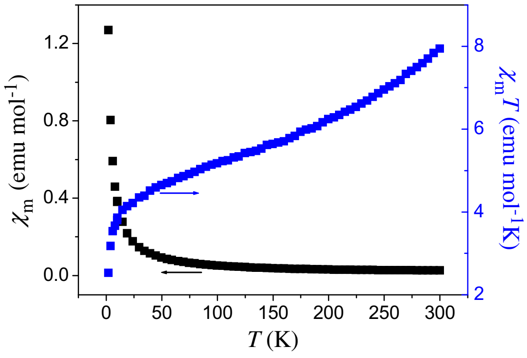

Fig. 4. Plots of χ_m vs. T and $\chi_m T$ vs. T for **5**.

4. Conclusions

Isolation of **1**, **2** and **5** demonstrates that *m*-ferrocenylbenzoate can stabilize lanthanide ions forming unique 1D *m*-ferrocenylbenzoate-bridged lanthanide coordination polymers. Electrochemical studies show that the steric effect of the *m*-ferrocenylbenzoates and the law of lanthanide contraction cooperatively affect the structures and electrochemical properties of **1**, **2** and **5**, whereas no obvious linear relationships are revealed between the structures and electrochemical properties of **1**–**5**. Magnetic investigations indicate that the structure of the *m*-ferrocenylbenzoate plays an essential role on the magnetic interactions between Gd(III) ions.

Acknowledgements

This work is financially supported by the National Natural Science Foundation of China (Nos. 20872030, 20972043 and 50903028), Heilongjiang Province (Nos. GC09A402 and 2009RFXXG201) and Heilongjiang University.

Appendix A. Supplementary material

CCDC Nos. 746793, 723155 and 760703 contain the supplementary crystallographic data for **1**, **2** and **5**, respectively. These data can be obtained free from The Cambridge Crystallographic Data Centre *via* www.ccdc.cam.ac.uk/data_request/cif.

References

[1] J. Jiang, D.K.P. Ng, Acc. Chem. Res. 42 (2009) 79–88.
[2] C. Benelli, D. Gatteschi, Chem. Rev. 102 (2002) 2369–2387.
[3] K. Binnemans, Chem. Rev. 109 (2009) 4283–4374.
[4] H.-X. Li, Y.-J. Zhu, M.-L. Cheng, Z.-G. Ren, J.-P. Lang, Q. Shen, Coord. Chem. Rev. 250 (2006) 2059–2092.
[5] D. Sun, R. Cao, Y. Liang, Q. Shi, M. Hong, J. Chem. Soc., Dalton Trans. (2002) 1847–1851.
[6] A. Thirumurugan, S. Natarajan, Dalton Trans (2004) 2923–2928.
[7] X. Guo, G. Zhu, Z. Li, F. Sun, Z. Yang, S. Qiu, Chem. Commun. (2006) 3172–3174.
[8] R. Shyni, S. Biju, M.L.P. Reddy, A.H. Cowley, M. Findlater, Inorg. Chem. 46 (2007) 11025–11030.
[9] M. Veith, A.L. Ndiaye, V. Huch, H. Cui, C. Wickleder, Z. Anorg. Allg. Chem. 634 (2008) 2551–2556.

[10] P. Yan, J. Xing, G. Li, W. Sun, J. Zhang, G. Hou, J. Coord. Chem. 62 (2009) 2095–2107.
[11] E.S. Andreiadis, R. Demadrille, D. Imbert, J. Pécaut, M. Mazzanti, Chem. Eur. J. 15 (2009) 9458–9476.
[12] B.V. Harbuzaru, A. Corma, F. Rey, J.L. Jordá, D. Ananias, L.D. Carlos, J. Rocha, Angew. Chem., Int. Ed. 48 (2009) 6476–6479.
[13] T.-H. Zhou, F.-Y. Yi, P.-X. Li, J.-G. Mao, Inorg. Chem. 49 (2010) 905–915.
[14] C. Policar, F. Lambert, M. Cesario, I. Morgenstern-Badarau, Eur. J. Inorg. Chem. (1999) 2201–2207.
[15] J.-M. Rueff, N. Masciocchi, P. Rabu, A. Sironi, A. Skoulios, Eur. J. Inorg. Chem. (2001) 2843–2848.
[16] J.-G. Wang, C.-C. Huang, X.-H. Huang, D.-S. Liu, Cryst. Growth Des. 8 (2008) 795–798.
[17] Q. Zhu, T. Sheng, R. Fu, S. Hu, J. Chen, S. Xiang, C. Shen, X. Wu, Cryst. Growth Des. 9 (2009) 5128–5134.
[18] Y.-Y. Yang, W.-T. Wong, Chem. Commun. (2002) 2716–2717.
[19] H. Hou, G. Li, L. Li, Y. Zhu, X. Meng, Y. Fan, Inorg. Chem. 42 (2003) 428–435.
[20] L. Li, J. Li, H. Hou, Y. Fan, Y. Zhu, Inorg. Chim. Acta 359 (2006) 3139–3146.
[21] V. Mereacre, A.M. Ako, G. Filoti, J. Bartolomé, C.E. Anson, A.K. Powell, Polyhedron 29 (2010) 244–247.
[22] P.F. Yan, F.M. Zhang, G.M. Li, J.W. Zhang, W.B. Sun, M. Suda, Y. Einaga, J. Solid State Chem. 182 (2009) 1685–1690.
[23] P. Hu, K. Zhao, L. Zhang, J. Si Chuan Normal Univ. (Nat. Sci.. Ed.) 21 (1998) 433–435 (in Chinese).
[24] G.M. Sheldrick, SHELXS-97, Program for Solution of Crystal Structures. University of Göttingen, Germany, 1997.
[25] G.M. Sheldrick, SHELXL-97, Program for Refinement of Crystal Structures. University of Göttingen, Germany, 1997.
[26] H. Hou, L. Li, G. Li, Y. Fan, Y. Zhu, Inorg. Chem. 42 (2003) 3501–3508.
[27] Z. Li, J. Li, G. Li, F. Zhang, J. Wu, G. Bao, Inorg. Chim. Acta 362 (2009) 3104–3108.
[28] X. Wang, Y. Liu, H. Hou, J. Wu, Y. Fan, J. Organomet. Chem. 694 (2009) 77–85.
[29] N. Das, A.M. Arif, P.J. Stang, Inorg. Chem. 44 (2005) 5798–5804.
[30] D. Guo, Y.-T. Li, C.-Y. Duan, H. Mo, Q.-J. Meng, Inorg. Chem. 42 (2003) 2519–2530.
[31] L. Liu, Z. Li, B. Wang, G. Li, L. Wang, X. Meng, Z. He, Cryst. Growth Des. 9 (2009) 5244–5258.
[32] G. Li, H. Hou, Y. Zhu, X. Meng, L. Mi, Y. Fan, Inorg. Chem. Commun. 5 (2002) 929–932.
[33] H. Hou, L. Li, Y. Zhu, Y. Fan, Y. Qiao, Inorg. Chem. 43 (2004) 4767–4774.
[34] J.A. Mata, E. Peris, J. Chem. Soc., Dalton Trans. (2001) 3634–3640.
[35] M.W. Cooke, T.S. Cameron, K.N. Robertson, J.C. Swarts, M.A.S. Aquino, Organometallics 21 (2002) 5962–5971.
[36] Z. Jin, K. Nolan, C.R. McArthur, A.B.P. Lever, C.C. Leznoff, J. Organomet. Chem. 468 (1994) 205–212.
[37] G.-L. Zheng, J.-F. Ma, Z.-M. Su, L.-K. Yan, J. Yang, Y.-Y. Li, J.-F. Liu, Angew. Chem., Int. Ed. 43 (2004) 2409–2411.
[38] R. Horikoshi, T. Mochida, H. Moriyama, Inorg. Chem. 41 (2002) 3017–3024.
[39] E.M. Barranco, O. Crespo, M.C. Gimeno, P.G. Jones, A. Laguna, M.D. Villacampa, J. Organomet. Chem. 592 (1999) 258–264.
[40] Y. Xu, P. Saweczko, H.-B. Kraatz, J. Organomet. Chem. 637–639 (2001) 335–342.